

BEHAVIOR OF LIGHT-GAUGE STEEL SHORT COLUMNS FILLED WITH NORMAL AND LIGHTWEIGHT AGGREGATE CONCRETE UNDER CONCENTRIC AXIAL LOADING

Ibrahim AL-Zubaidi¹, Mu'tasim Abdel-Jaber^{2,†}, Yasser M. Hunaiti¹, Rola El-Nimri^{1*}

¹ Department of Civil Engineering, The University of Jordan, Amman, Jordan

² Department of Civil Engineering, Al-Ahliyya Amman University, Amman, Jordan

[†] On sabbatical leave from Department of Civil Engineering, The University of Jordan, Amman, Jordan

*rola.elnimri@gmail.com

This study aims to investigate experimentally and numerically the behavior of light-gauge steel tubes filled with normal and lightweight concrete under axial loading. A total of thirty-five specimens, including thirty-two composite columns, two bare steel columns, and one normal-weight plain concrete column, were considered. The main variables in the tests were the concrete infill type (normal-weight and lightweight), the column's length (1, 1.25, 1.5, 1.75-m), the steel tube thickness (2 and 2.4-mm), and the cross-section (100×100 and 150×150-mm). In addition, theoretical capacities were computed according to Eurocode 4, and a finite element analysis was conducted using ABAQUS software. The results showed that the behavior of lightweight filled steel tubes was similar to the normal weight filled tubes during the test; however, their capacities were lower compared to the normal weight filled tubes by a range of (1%-20%). Yet, lightweight filled steel tubes can achieve high axial loads. In addition, the axial capacity of all composite columns decreased with the increase of the column's height and increased with the increase of both the cross-section and the steel thickness. Current code specifications of EC4 and the numerical results obtained from ABAQUS overestimated the capacities of the composite concrete-filled tubes by 3% and 14%, respectively; however, the EC4 was found to present close estimations to the experimental results.

Keywords: light-gauge steel, lightweight concrete, composite action, finite element analysis

List of Notations

CFST: Concrete-filled Steel Tube

LWA: lightweight aggregate

w/c: water-to-cement ratio

$N_{pl,Rd}$: plastic resistance of the composite section

A_s : area of steel tube

f_y : yield stress of steel

A_c : area of concrete core

f'_c : compressive strength of concrete

N_e : buckling load

$(E)_e$: effective flexural stiffness

l_e : effective length

1 INTRODUCTION

When hollow steel elements encounter external loads, local buckling of steel might take place if the dimension to thickness ratio is too high. By filling the hollow steel with concrete infill, the potential of steel buckling is reduced. These elements are called Concrete-filled Steel Tube (CFST) structures. Although the concrete core enhances the strength of the steel tube and avoids buckling, the steel tube also acts as longitudinal and lateral reinforcement for the concrete core providing confinement that helps it resisting tension, bending moment, and shear forces. The advantages of CFST structures over other composite systems include: the steel tube provides formwork for the concrete, the concrete prolongs local buckling of the steel tube wall, the steel tube prohibits excessive concrete spalling, and it adds significant stiffness to a frame compared to traditional steel frame construction [1]. Several researches were conducted to study the behavior of CFST composite beams [2–4], filled with recycled concrete [5–6], under acid attack [7], with unequal double spans [8], narrow width girders [9], and cold formed steel [10–11], in addition to the bond strength of composite columns [12] and the behavior of composite columns filled with high strength concrete [13–14], normal concrete [15–17], foamed and lightweight concrete [18], recycled concrete [19–20], and made with light gauge steel [21–23]. The main conclusions -proved that the CFST's recorded higher ductility and strength compared to the hollow steel sections in which both composite beams and columns sustained larger deformations. In addition, composite columns did not record any buckling of the tube's wall; hence, the failure was governed by the crushing of concrete and the yielding of the steel tube. Moreover, the current specifications of the EUROCODE 4 (EC4) conservatively estimated the strength of CFST beams and columns. Cortés-Puentes W. et al.

[21], investigated experimentally the compressive strength of light-gauge steel composite columns. Fourteen stub columns and twelve full scale columns were considered with width-to-thickness ratio of 125. The tested stub columns consisted of concrete only columns, steel only columns, confined concrete columns, and composite columns to assess the effect of confinement, local buckling, and the individual contributions of each component to the axial capacity. Enhancement has been seen, in capacity of 16% due to confinement; however, its effect was negligible for full-scale columns, whereas the load capacity of full-scale columns was found to be proportional to the cross-sectional area. Local buckling controlled the strength of steel only columns, where the steel section's capacity reached 33% of its tensile capacity.

On the other hand, the weight of a structure plays a major role in the design process. The lower the self-weight, i.e., the dead load, the smaller the stresses that the element encounter; thus, smaller sections can be used to sustain similar live loads [24]. This can be achieved in CFST by changing the concrete filling from normal weight concrete to lightweight aggregate (LWA) concrete. In 2010, Ghannam S. et al. [25] studied the behavior of eight full scale rectangular columns filled with normal and lightweight concrete. Two slenderness ratios were considered; 20 and 25. The authors stated that high columns' strength was achieved with reduction in weight. Salgar P. B. and Patil P.S. [26] conducted tests on sixty-four struts up to failure to examine the axial behavior of lightweight CFST. Different lengths, sectional sizes, and thicknesses were considered in the study. The results indicated that using lightweight concrete as infill reduced the weight of the specimens by 25% compared to struts filled with normal concrete. The axial strength of CFT specimen increased as the depth to thickness (D/t) ratio decreased for similar slenderness ratios. Similarly, the capacity decreased as the slenderness ratio was increased.

In light of the above-mentioned literature, this study aims to investigate the behavior of light-gauge steel columns filled with normal and lightweight aggregate concrete. The significance of this study comes from combining the advantages of filling the empty steel tubes by lighter concrete, which would help reducing the total weight and obtaining smaller sections. A total of thirty-five specimens were tested divided into three categories: thirty-two composite columns, two empty steel columns, and one normal-weight plain concrete column. Two steel thicknesses (2 and 2.4-mm), two square cross-sections (100 and 150-mm), and four columns' lengths (1, 1.25, 1.5, and 1.75-m) were considered. Moreover, the theoretical capacities were calculated according to EC4 [27], and a finite element analysis was conducted using ABAQUS software to predict and compare the axial strength with the experimental results.

2 MATERIALS

2.1 Cement

ordinary Portland - Pozzolana Cement (CEM II/A-P 42.5N) was used in compliance with the Jordanian Code of JS30-1:2007 and the European Code EN197-1:2000. The cement had a specific gravity of 3100 kg/m³, and an initial setting time of 150 minutes.

2.2 Aggregates

2.2.1 Normal Weight Aggregates

Crushed limestone was used as coarse aggregates in this study, having a maximum size of 20-mm. The aggregates were sieved according to the ACI E-701 [28] to get their gradation ranging between sieve number 20 and sieve number 4. Water absorption and bulk density were tested according to ASTM C127 [29] and the results are illustrated in Table 1.

2.2.2 Lightweight Aggregates

The LWA used in this study were tuff stone with an abrasion value of 38%. Water absorption and bulk density were also tested according to ASTM C127 [29] and the results are shown in Table 1.

Table 1. Coarse Aggregates Properties

Property	Normal Weight Aggregates	Lightweight Aggregates
Water Absorption %	1.23	11
Bulk Density (Unit Weight kg/m ³)	1669	636

2.2.3 Fine Aggregates

Silica sand was used from local sources, containing mineral particles with a diameter ranging between 0.06 and 2.0-mm.

2.3 Light-Gauge Steel

Light-gauge steel is also called cold-formed steel is used in this study. Two steel thicknesses were considered: 2 and 2.4-mm. The steel tubes were formed without any heat exposure, i.e., at room temperature. To protect the steel from corrosion, the steel sheets were coated with zinc. Yield strength, tensile strength, and elongation tests were performed according to ASTM A370 [30] and the results are reported in Table 2.

Table 2: Properties of Steel

Sample	Yield Strength - f_y (MPa)	Tensile Strength - f_u (MPa)
t = 2 mm	220.1	350.2
t = 2.4 mm	219.6	353.4

3 EXPERIMENTAL PROGRAM

3.1 Details of Mix Proportions

Both the control mix and lightweight concrete mix were designed according to the ACI 318-19 [31] to reach a compressive strength of 30-MPa after 28-days of casting and curing. Both mixes had a water-to-cement ratio (w/c) of 0.48. Table 3 shows the mix proportions and compressive strength of each mix. To obtain the compressive strength of concrete, six cubes of 150×150×150-mm are taken from each batch in which two cubes were tested at 7-days and the others were tested at 28-days of curing.

Table 3: Concrete Mix Proportions and Compressive Strength

Mix	Coarse Aggregates (kg/m ³)	Fine Aggregates (kg/m ³)	Cement (kg/m ³)	Water (kg/m ³)	w/c	f_{cu} (MPa)	
						7-days	28-days
Control	1145	638	375	180	0.48	26.79	Control
Lightweight	636	656	450	216	0.48	25.17	Lightweight

3.2 Preparation of Columns

The steel tubes were prepared by welding two steel plates using an Exx70 weld type with 3 mm weld thickness and placed on a wooden floor to ensure that no concrete leakage could take place from the bottom side. The concrete was then poured inside the steel tube in three layers, with each layer compacted for 25-stroke using a long steel rod to avoid any segregation and eliminate all the air voids.

3.3 Column's Geometry

All columns had a square cross-section; however, the sections differed in size and steel thickness. Figure 1 illustrates the sections' sizes, geometry, and steel sheet detailing. Two sections were considered: (100×100) and (150×150)-mm square sections with two different steel thicknesses for each section: 2 and 2.4-mm, and four columns' lengths: 1, 1.25, 1.5, and 1.75-m.

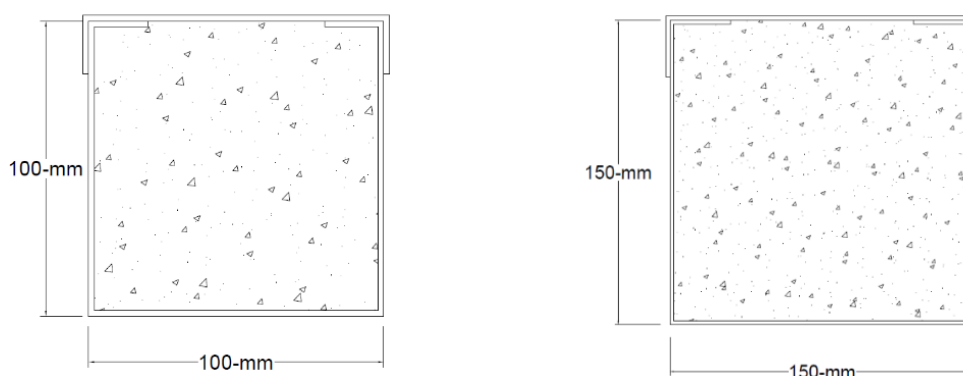


Fig. 1. Cross-Sections; (a) 100-mm Cross-Section; (b) 150-mm Cross-Section.

3.4 Specimen's Details

A Total of thirty-five columns were tested in this research divided into eight groups based on the cross-section dimensions, steel thickness, and concrete infill. Two additional groups were also considered; group 9 and 10, which refers to empty steel columns and one plain concrete column, respectively. Table 4 illustrates the groups and specimen's labels. The columns were labeled in an order of (Type of concrete infill – Steel thickness – cross-sectional dimension – column's length). For example, the specimen LW-2-10-175 refers to a 100-mm square column with 2-mm steel thickness and 1.75-m length filled with lightweight concrete. On the other hand, group 9, which refers to the group containing 1-m length empty steel columns were labeled as (S – steel thickness). For example, S-2.4 refers to a bare-steel column with 2.4-mm steel thickness. Finally, group 10, contains one column labeled as C that refers to a plain concrete column with a 1-m length.

Table 4: Specimens' Details and labeling

Cross-Section Dimension (mm)	Steel Thickness (mm)	Length (m)	Concrete Infill	Group Number	Column's Label	
100	2	1	Normal	1	NW-2-10-100	
		1.25			NW-2-10-125	
		1.5			NW-2-10-150	
		1.75			NW-2-10-175	
		1	Lightweight	2	LW-2-10-100	
		1.25			LW-2-10-125	
		1.5			LW-2-10-150	
		1.75			LW-2-10-175	
	2.4	1	Normal	3	NW-2.4-10-100	
					1.25	NW-2.4-10-125
					1.5	NW-2.4-10-150
					1.75	NW-2.4-10-175
		1	Lightweight	4	LW-2.4-10-100	
					1.25	LW-2.4-10-125
					1.5	LW-2.4-10-150
					1.75	LW-2.4-10-175
150	2	1	Normal	5	NW-2-15-100	
					1.25	NW-2-15-125
					1.5	NW-2-15-150
					1.75	NW-2-15-175
		1	Lightweight	6	LW-2-15-100	
					1.25	LW-2-15-125
					1.5	LW-2-15-150
					1.75	LW-2-15-175
	2.4	1	Normal	7	NW-2.4-15-100	
					1.25	NW-2.4-15-125
					1.5	NW-2.4-15-150
					1.75	NW-2.4-15-175
		1	Lightweight	8	LW-2.4-15-100	
					1.25	LW-2.4-15-125
					1.5	LW-2.4-15-150
					1.75	LW-2.4-15-175
Empty Steel	2	1	-	9	S-2	
	2.4	1	-		S-2.4	
Plain Concrete	-	1	Normal	10	C	

3.5 Test Setup

All columns were supported at the bottom end with a steel plate connected to the ground while the top end of the columns was free. The columns were subjected to an increasing axial force applied using a DARTEC- universal-testing machine with a capacity of 2000 kN. Figure 2 illustrates the test setup.

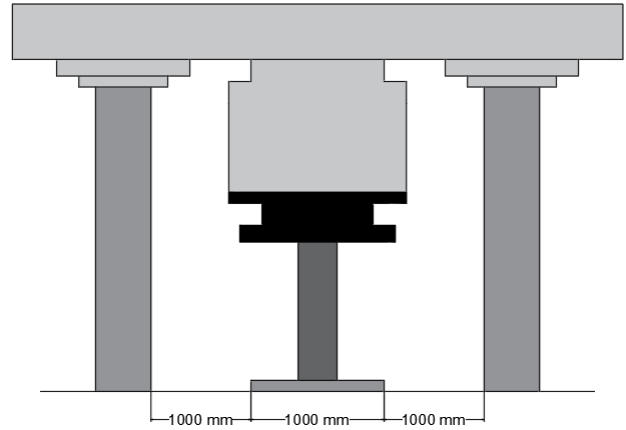


Fig. 2. Test Setup

4 RESULTS AND DISCUSSION

4.1 General Behavior and Failure Modes

All composite columns filled with both normal and lightweight concrete failed in a similar manner, which was represented by the local buckling of steel tube and crushing of concrete core at either one end or both ends of the column. The same observation was reported by Salgar P. B. and Patil P.S. [26]. In hollow steel columns, the inward and outward deformation occurred at both ends; however, the inward deformation was prevented by the concrete infill in composite columns. For the concrete only column, hair cracks initiated near the bottom end and propagated until they reached approximately the column's mid-height. Figure 3 shows the failure modes of all columns.



(a) NW-2.4-15-100



(b) NW-2.4-10-125



(c) NW-2-10-175



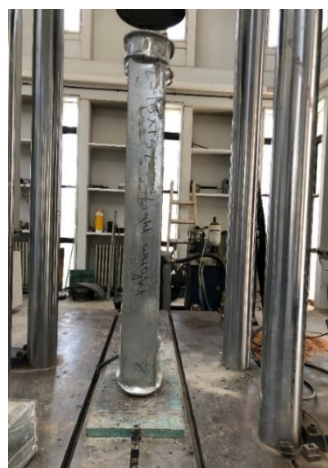
(d) Concrete Core Crushing



(e) LW-2.4-15-150



(f) LW-2.4-10-125



(g) LW-2-15-175



(h) Empty Steel Columns



(i) Plain Concrete Column

Fig. 3. Failure Modes of Columns

4.2 Experimental Capacity

The experimental axial carrying capacities of all columns were obtained from the test and the results are shown in Table 5. Specimens (NW-2-10-150, LW-2-10-150, NW-2-15-125, and LW-2-15-125) showed abnormal values and patterns than other specimens; thus, the results were eliminated.

Table 5: Experimental Capacities of All Columns

Steel Thickness (mm)	Length (m)	100x100-mm		150x150-mm	
		Column's Label	Experimental Capacity (kN)	Column's Label	Experimental Capacity (kN)
2	1	NW-2-10-100	495	NW-2-15-100	948
	1.25	NW-2-10-125	485	NW-2-15-125	-
	1.5	NW-2-10-150	-	NW-2-15-150	859
	1.75	NW-2-10-175	470	NW-2-15-175	832
	1	LW-2-10-100	412	LW-2-15-100	870
	1.25	LW-2-10-125	409	LW-2-15-125	-
	1.5	LW-2-10-150	-	LW-2-15-150	739
	1.75	LW-2-10-175	401	LW-2-15-175	700
2.4	1	NW-2.4-10-100	588	NW-2.4-15-100	1041
	1.25	NW-2.4-10-125	554	NW-2.4-15-125	970
	1.5	NW-2.4-10-150	519	NW-2.4-15-150	933
	1.75	NW-2.4-10-175	513	NW-2.4-15-175	864
	1	LW-2.4-10-100	516	LW-2.4-15-100	982
	1.25	LW-2.4-10-125	512	LW-2.4-15-125	953
	1.5	LW-2.4-10-150	495	LW-2.4-15-150	871
	1.75	LW-2.4-10-175	412	LW-2.4-15-175	852
2	1	S-2	163		
2.4	1	S-2.4	265		
-	1	C	305		

4.2.1 Effect of Column's Length

The capacity of all columns decreased with the increase of the column's length; however, this reduction in capacity increased with increasing the steel thickness and the cross-sectional size. This can be attributed to the fact that by increasing the steel thickness or the section size, the portion of load carried by the steel increases, and according to

the specifications the failure of steel under compression is critical due to the local buckling; thus, the reduction in capacity increases.

For 100×100-mm sectional size, the reduction in capacity was ranging between (1%-5%) and (1%-20%) for 2 and 2.4-mm steel thickness, respectively. On the other hand, for 150×150-mm sectional size, the reduction in capacity was (9%-20%) and (3%-17%) for 2 and 2.4-mm steel thickness, respectively.

Further, for 2-mm steel thickness, the reduction in capacity was ranging between (1%-5%) and (9%-20%) for 100×100 and 150×150-mm sectional size, respectively, while it was (1%-20%) and (3%-17%) for the same sectional sizes mentioned, respectively. Figure 4 illustrates the change in columns' capacity with its length.

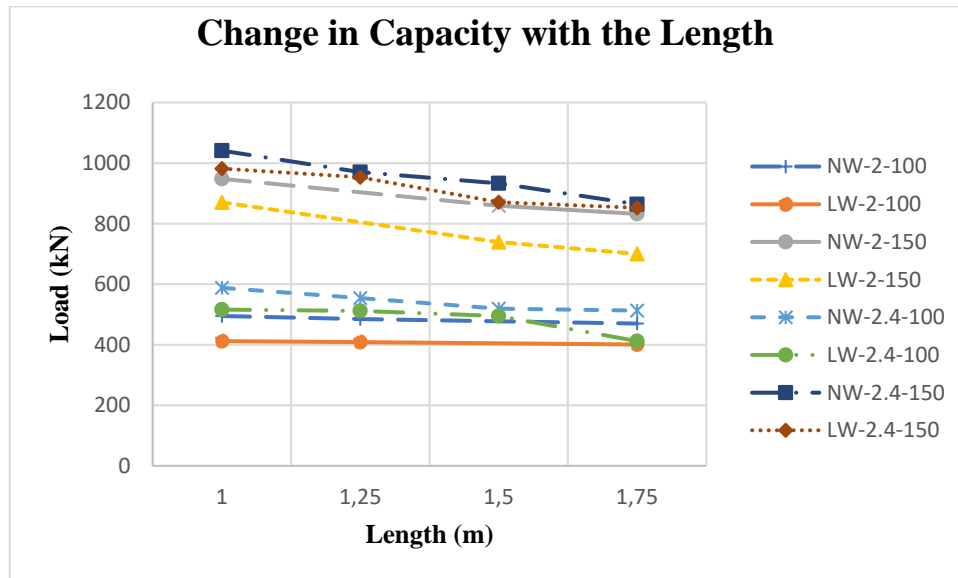


Fig. 4. Change in Capacity with the Columns' Length

4.2.2 Effect of Concrete Infill Type

In all groups, and for the same column's height, the capacity of the column filled with normal-weight concrete was higher than their corresponding column filled with lightweight concrete. This reduction decreased with increasing the section size. For 100×100-mm cross-section, the capacity decreased by (15%-17%) and (5%-20%) for 2- and 2.4-mm steel thicknesses, respectively. However, for 150×150-mm cross-section, the reduction in capacity was ranging between (8%-16%) and (1%-7%) for 2- and 2.4-mm steel thicknesses, respectively. The results match the same conclusions reported by Ghannam S. et al. [25]. Figure 5 represents a comparison between the normal-weight and lightweight filled steel tubes.

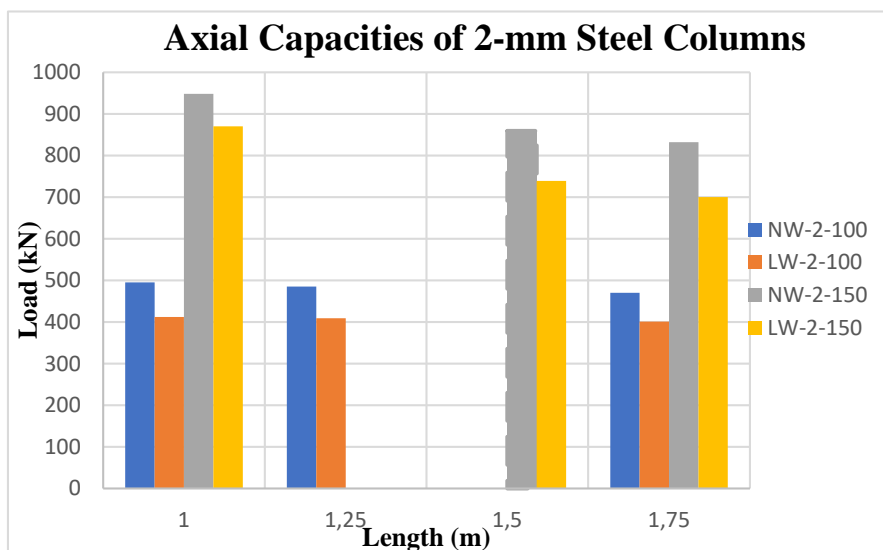


Fig. 5. Axial Capacity of Columns; (a) 2-mm Steel Thickness;

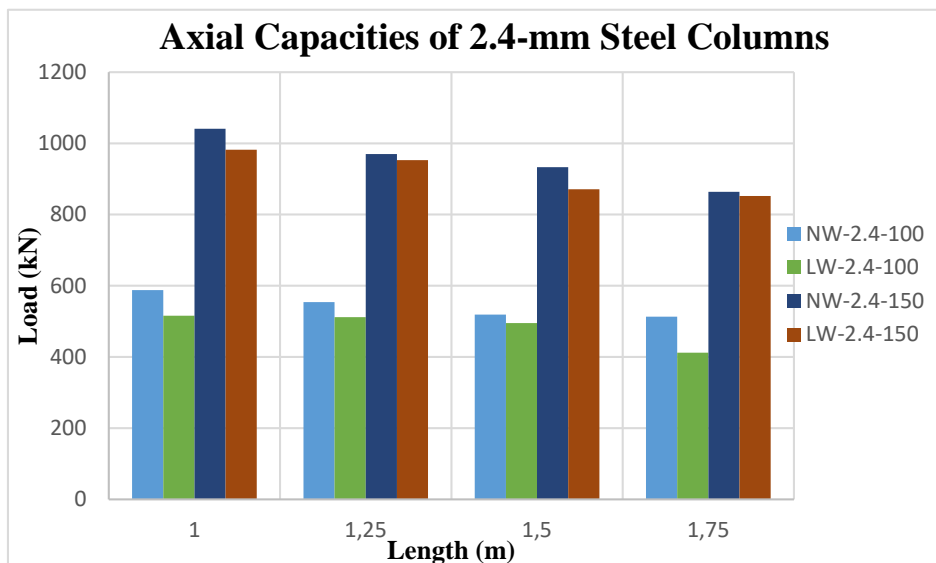


Fig. 5. Axial Capacity of Columns; (b) 2.4-mm Steel Thickness

4.2.3 Effect of Steel Thickness

The Axial capacity increased with increasing the thickness of the steel tube. For normal weight filled columns with the same height, the axial capacity increased more than its corresponding lightweight filled column. However, this increment decreased with increasing the section size. The capacities of 2.4-mm normal-weight steel filled columns were (8%-16%) and (4%-9%) higher than the capacities of their corresponding 2-mm steel columns for 100×100 and 150×150-mm section sizes, respectively, while for lightweight filled steel columns, the percentages were (3%-20%) and (11%-18%) for the previously mentioned sections, respectively.

4.2.4 Effect of Section Size

Both the normal and lightweight concrete filled steel columns had a similar trend, in which their capacity increased with increasing the section size. The columns with 150×150-mm cross-section recorded higher capacities than the columns with 100×100-mm cross-section by a range of (68%-111%).

5 FINITE ELEMENT ANALYSIS (FEA) BY ABAQUS

5.1 Modelling

5.1.1 Materials

The elasticity of both steel and concrete was defined with a poisson's ratio of 0.3 and 0.2, respectively. Steel was defined as a plastic material, while the plasticity of concrete was defined using the Concrete Damage Plasticity (CDP) model with plasticity parameters defined according to ABAQUS user guide manual [32]. The compressive and tensile stress-strain behaviors of concrete were obtained according to Tsai's equations [33] and are illustrated in Figure 6.

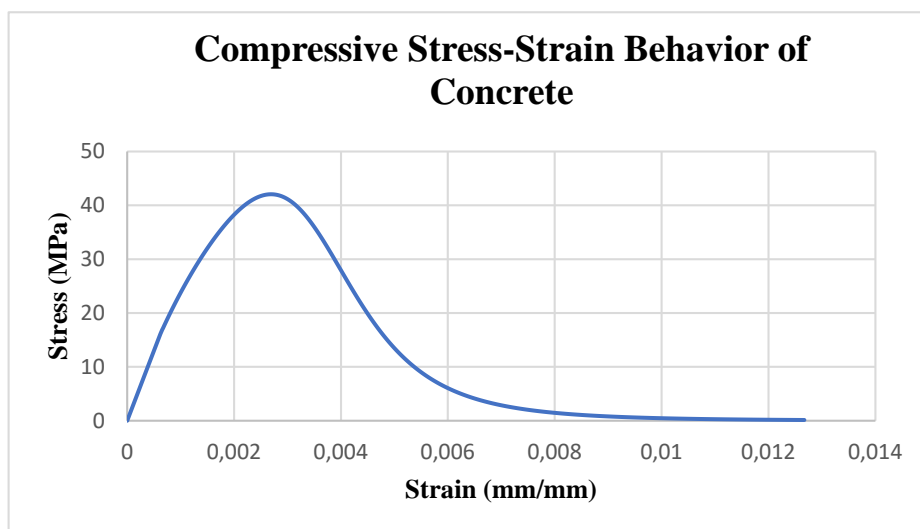


Fig.6. Stress-Strain Relationship of Concrete; (a) Compressive Stress-Strain Diagram;

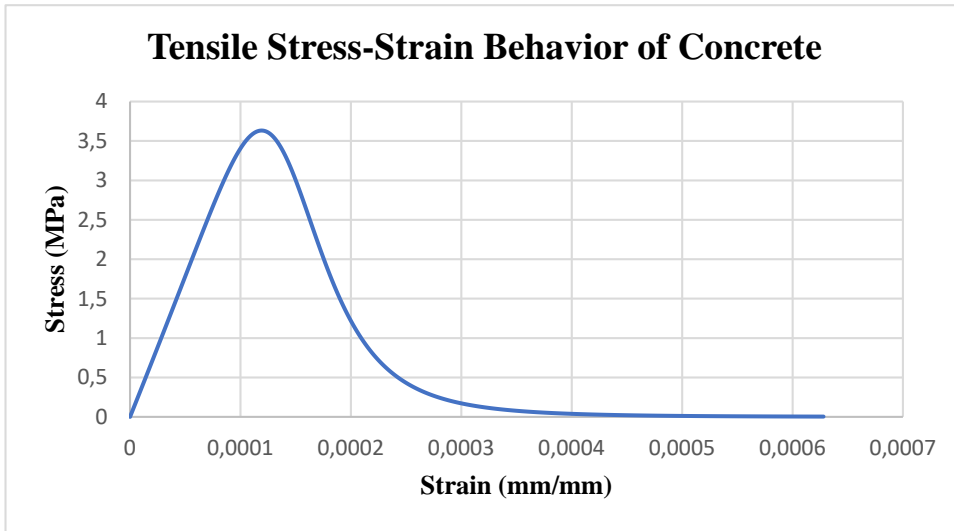


Fig.6. Stress-Strain Relationship of Concrete; (b) Tensile Stress-Strain Diagram

5.1.2 Sections

Sections are used to link each part with its corresponding material. For this model, two sections were defined as a solid homogeneous type and associated with one of the predefined materials. After that, each part was linked with its corresponding section. However, the discrete rigid plate was not assigned to any section due to its definition.

5.1.3 Meshing, Interactions, and Boundary Conditions

the steel tube and the concrete core, were meshed with a size of 30 mm and assigned to 3D stress family with C3D8R element type, while the steel plate was meshed with a size of 20 mm and assigned to discrete rigid element family with R3D4 element type. All parts were assigned to hexahedral-shaped element and meshed before the assembly of the model. Table 6 illustrates all parts' details and Figure 7 shows the model and meshed parts in ABAQUS.

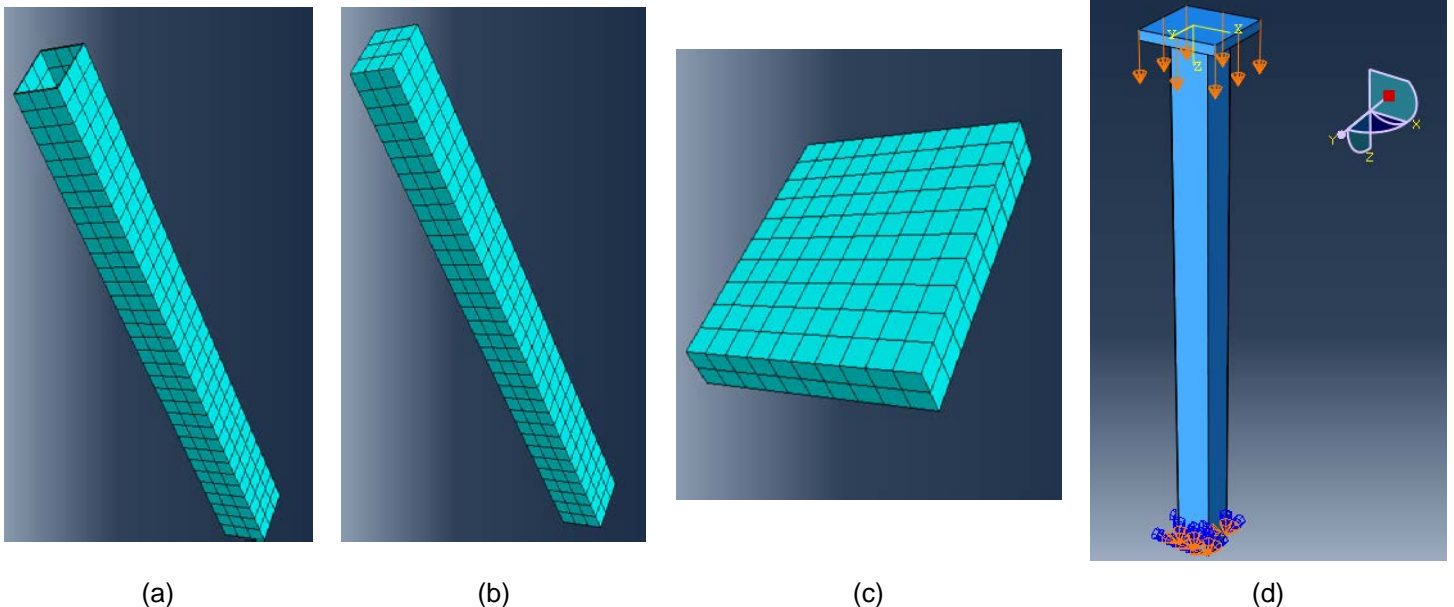


Fig. 7. FE Model; (a) Steel Tube; (b) Concrete Core; (c) Steel Plate; (d) Assembled Model

Table 6: ABAQUS Parts' details

Part	Mesh Size (mm)	Mesh Shape	Family	Element Type
Steel Tube	30	hexahedral	3D stress	C3D8R
Concrete Core	30	hexahedral	3D stress	C3D8R
Plate	20	hexahedral	discrete rigid	R3D4

Surface-to-surface interaction was created between the steel tube's internal faces and the concrete core's external faces with a friction coefficient of 0.3 and a hard contact property. This is to ensure that all parts will act as one body when applying the load.

The top end of the column was designed to move in the axial direction only with constraining all types of movements and rotations. The bottom end was fully fixed to simulate the actual setup.

A dynamic explicit step was defined to apply the displacement to the column, this test is applicable as long as the kinetic energy is maintained to almost zero. The maximum displacement was applied to the discrete rigid plate using the boundary conditions with a smooth step amplitude. After the analysis, the axial capacity was obtained and compared to the experimental results.

5.2 FEA Results

The FEA was conducted using ABAQUS software and the results are illustrated in Table 7. ABAQUS was not conservative with predicting the axial capacity of composite columns, as the results were around 14% higher than the experimental ones. The difference between the experimental results and ABAQUS results increased with increasing the column's length. This could be due to the confinement and interaction between the steel tube and concrete core.

Table 7: FEA Results

Column's Label	P_{exp} (kN)	P_{ABAQUS} (kN)	P_{ABAQUS} / P_{exp}
NW-2-10-100	495	490	0.99
NW-2-10-125	485	489	1.01
NW-2-10-150	-	-	-
NW-2-10-175	470	492	1.05
LW-2-10-100	412	441	1.07
LW-2-10-125	409	442	1.08
LW-2-10-150	-	-	-
LW-2-10-175	401	443	1.10
NW-2.4-10-100	588	527	0.90
NW-2.4-10-125	554	525	0.95
NW-2.4-10-150	519	521	1.00
NW-2.4-10-175	513	518	1.01
LW-2.4-10-100	516	521	1.01
LW-2.4-10-125	512	521	1.02
LW-2.4-10-150	495	522	1.05
LW-2.4-10-175	412	519	1.26
NW-2-15-100	948	1159	1.22
NW-2-15-125	-	-	-
NW-2-15-150	859	1155	1.34
NW-2-15-175	832	1153	1.39
LW-2-15-100	870	997	1.15
LW-2-15-125	-	-	-
LW-2-15-150	739	987	1.34
LW-2-15-175	700	989	1.41
NW-2.4-15-100	1041	1185	1.14
NW-2.4-15-125	970	1207	1.24
NW-2.4-15-150	933	1203	1.29
NW-2.4-15-175	864	1215	1.41
LW-2.4-15-100	982	1088	1.11
LW-2.4-15-125	953	1032	1.08
LW-2.4-15-150	871	1034	1.19
LW-2.4-15-175	852	1031	1.21
Mean			1.14
coefficient of variation			0.126
Reduction Percent (%)			-14%

6 CAPACITY CALCULATIONS ACCORDING TO EUROCODE 4

6.1 Equations

The axial capacities of composite columns were calculated according to the EC4 [27] using the following equations:

$$N_{pl,Rd} = A_s F_y + 0.85 A_c f'_c \quad (1)$$

$$N_e = \pi^2 \frac{(EI)_e}{l_e^2} \quad (2)$$

Where $N_{pl,Rd}$ is the plastic resistance of the composite section, A_s is the area of steel tube, f_y is the yield stress of steel, A_c is the area of concrete core, f'_c is the compressive strength of concrete, N_e is the buckling load, $(EI)_e$ is the effective flexural stiffness, and l_e is the effective length.

6.2 Eurocode 4 Results

The EC4 [27] was used to predict both the buckling load and the axial capacity of all composite columns. Table 8 presents the theoretical capacities of composite columns obtained according to the EC4 [27].

Table 8: Theoretical Capacities According to EC4

Column's Label	P_{exp} (kN)	Theoretical Capacity (kN)		P_u / P_{exp}	$P_{Buckling}/P_{exp}$
		P_u	$P_{Buckling}$		
NW-2-10-100	495	488	3093	0.99	6.25
NW-2-10-125	485	488	1979	1.01	4.08
NW-2-10-150	-	-	-	-	-
NW-2-10-175	470	488	1010	1.04	2.15
LW-2-10-100	412	432	3093	1.05	7.51
LW-2-10-125	409	432	1979	1.06	4.84
LW-2-10-150	-	-	-	-	-
LW-2-10-175	401	432	1010	1.08	2.52
NW-2.4-10-100	588	524	3694	0.89	6.28
NW-2.4-10-125	554	524	2364	0.95	4.27
NW-2.4-10-150	519	524	1641	1.01	3.16
NW-2.4-10-175	513	524	1206	1.02	2.35
LW-2.4-10-100	516	470	3694	0.91	7.16
LW-2.4-10-125	512	470	2364	0.92	4.62
LW-2.4-10-150	495	470	1641	0.95	3.32
LW-2.4-10-175	412	470	1206	1.14	2.93
NW-2-15-100	948	958	10529	1.01	11.11
NW-2-15-125	-	-	-	-	-
NW-2-15-150	859	958	4679	1.12	5.45
NW-2-15-175	832	958	3438	1.15	4.13
LW-2-15-100	870	831	10529	0.96	12.10
LW-2-15-125	-	-	-	-	-
LW-2-15-150	739	831	4679	1.12	6.33
LW-2-15-175	700	831	3438	1.19	4.91
NW-2.4-15-100	1041	1014	12592	0.97	12.10
NW-2.4-15-125	970	1014	8059	1.05	8.31
NW-2.4-15-150	933	1014	5596	1.09	6.00
NW-2.4-15-175	864	1014	4111	1.17	4.76
LW-2.4-15-100	982	888	12592	0.90	12.82
LW-2.4-15-125	953	888	8059	0.93	8.46
LW-2.4-15-150	871	888	5596	1.02	6.42
LW-2.4-15-175	852	888	4111	1.04	4.83

Mean

1.03

6.04

Column's Label	P_{exp} (kN)	Theoretical Capacity (kN)		P_u / P_{exp}	$P_{Buckling} / P_{exp}$
		P_u	$P_{Buckling}$		
coefficient of variation				0.081	0.490
Reduction Percent (%)				-3%	-504%

According to the EC4, buckling of columns will occur at high loads due to the slenderness of the test specimens; hence, the failure of composite columns will be caused by concrete crushing and steel local buckling. This confirms well with the outcomes of this study. The maximum axial capacities predicted by EC4 were around 3% higher than the experimental results; thus, the EC4 was not conservative in predicting the capacities. This can be attributed to the fact that the predicted capacities according to the EC4 depends only on the cross-section without considering the effect of the column's length, as it was seen that the capacity decreased with increasing the column's length.

7 CONCLUSIONS

It can be concluded from the results of this research that all composite columns, regardless of the concrete infill type, showed similar behavior during the test and failed in a similar manner.

Although the axial capacity of lightweight CFST's was lower than their corresponding normal-weight composite columns by a range of (1%-20%), high axial loads can be achieved. However, the axial capacity decreased with increasing the column's height by (1%-20%) and (3%-17%) for 100x100 and 150x150 mm sections., respectively, and increased with increasing both the cross-section and the steel tube's thickness by (68%-111%) and (3%-20%), respectively.

Both the concrete core and the steel tube enhanced the behavior and capacity of each other by (95%-204%) and (2%-93%), respectively. The concrete infill delayed the local buckling of the steel tube, and the steel sheets increased the axial capacity of the plain-concrete column and changes its failure from brittle to ductile.

Although the EC4, in general, was found to overestimate the axial capacities of composite columns; however, its results were found to be close to the experimental capacities, as the difference between the theoretical and experimental capacities was about 3% only. On the other hand, the numerical capacities predicted by ABAQUS software were found to overestimate the axial capacities of composite columns by about 14%.

8 ACKNOWLEDGEMENTS

The authors would like to thank Deanship of Academic Research at The University of Jordan for their financial support to perform this research.

9 REFERENCES

- [1] Patidar, A.K. (2012). Behaviour of Concrete Filled Rectangular Steel Tube Column. IOSR J. Mech. Civ. Eng. 4, 46–52. <https://doi.org/10.9790/1684-0424652>.
- [2] Soundararajan, A., Shanmugasundaram, K. (2008). Flexural behaviour of concrete-filled steel hollow sections beams. J. Civ. Eng. Manag. 14, 107–114. <https://doi.org/10.3846/1392-3730.2008.14.5>.
- [3] Han, L.H. (2004). Flexural behaviour of concrete-filled steel tubes, J. Constr. Steel Res. 60, 313–337. <https://doi.org/10.1016/j.jcsr.2003.08.009>.
- [4] Flor, J.M. Fakury, R.H. Caldas, R.B. Rodrigues, F.C. Araújo, A.H.M. (2017). Experimental study on the flexural behavior of large-scale rectangular concrete-filled steel tubular beams. Rev. IBRACON Estruturas e Mater. 10, 895–905. <https://doi.org/10.1590/s1983-41952017000400007>.
- [5] El-Nimri, R., Abdel-Jaber, M.S., Hunaiti, Y.M., Abdel-Jaber, M., Behavior of light-gauge steel beams filled with recycled concrete, Mag. Civ. Eng. 101 (2021). <https://doi.org/10.34910/MCE.101.2>.
- [6] Yang, Y.F. Man, L.H. (2006) Compressive and flexural behaviour of recycled aggregate concrete filled steel tubes (RACFST) under short-term loadings, Steel Compos. Struct. 6, 257–284. <https://doi.org/10.1016/j.jlumin.2005.09.005>.
- [7] Xie, L. Chen, M. Sun, W. Yuan, F. Huang, H. (2019). Behaviour of concrete-filled steel tubular members under pure bending and acid rain attack: Test simulation, Adv. Struct. Eng. 22, 240–253. <https://doi.org/10.1177/1369433218783323>.
- [8] Fong, M. Chan, S.T. Chan, S.L. (2011). Capacities of Concrete-filled Steel Beams of Unequal Double Spans by Testing and Code, HKIE Trans. Hong Kong Inst. Eng. 18, 1–5. <https://doi.org/10.1080/1023697X.2011.10668217>.
- [9] Nakamura, S. ichi. Morishita, H. (2008). Bending strength of concrete-filled narrow-width steel box girder, J. Constr. Steel Res. 64, 128–133. <https://doi.org/10.1016/j.jcsr.2007.03.001>.
- [10] Jyothi K. N, Valsa Ipe . T, (2015). Performance of Infilled Cold Formed Steel Channel Section Beams, Int. J. Eng. Res. V4 446–451. <https://doi.org/10.17577/ijertv4is120523>.

- [11] Valsa Ipe, T. Sharada Bai, H. Manjula Vani, K. Iqbal, M.M.Z. (2013). Flexural behavior of cold-formed steel concrete composite beams, *Steel Compos. Struct.* 14, 105–120. <https://doi.org/10.12989/scs.2013.14.2.105>.
- [12] Hunaiti, Y.M. (1991). BOND STRENGTH IN BATTENED COMPOSITE COLUMNS, 117, 699–714.
- [13] Zhang, S. Guo, L. Ye, Z. Wang, Y. (2005). Behavior of steel tube and confined high strength concrete for concrete-filled RHS tubes, *Adv. Struct. Eng.* 8, 101–116. <https://doi.org/10.1260/1369433054037976>.
- [14] L. H. H., T. T. C. H., Load Carrying Capacity of High Strength Cold-Formed Steel Built-Up Box Sections, 1 (2012) 494–499. https://doi.org/10.3850/978-981-08-6218-3_ss-th016.
- [15] De Nardin, S. El Debs, A.L.H.C. (2007). Axial load behaviour of concrete-filled steel tubular columns, *Proc. Inst. Civ. Eng. Struct. Build.* 160, 13–22. <https://doi.org/10.1680/stbu.2007.160.1.13>.
- [16] Kuranovas, A. Goode, D. Kvedaras, A.K Zhong, S. (2009). Load-bearing capacity of concrete-filled steel columns, *J. Civ. Eng. Manag.* 15, 21–33. <https://doi.org/10.3846/1392-3730.2009.15.21-33>.
- [17] Sakino, K. Nakahara, H. Morino, S. Nishiyama, I. (2004). Behavior of Centrally Loaded Concrete-Filled Steel-Tube Short Columns, *J. Struct. Eng.* 130, 180–188. [https://doi.org/10.1061/\(asce\)0733-9445\(2004\)130:2\(180\)](https://doi.org/10.1061/(asce)0733-9445(2004)130:2(180)).
- [18] Hunaiti, Y.M. (1996). COMPOSITE ACTION OF FOAMED AND LIGHTWEIGHT AGGREGATE CONCRETE, 8, 111–113.
- [19] Eltaly, B. Bembawy, A. Meleka, N. Kandil, K. (2017). Structural behavior of recycled aggregates concrete filled steel tubular columns, *Chall. J. Concr. Res. Lett.* 8, 17. <https://doi.org/10.20528/cjcr.2017.01.003>.
- [20] Yang, Y.F. Ma, G.L. (2013). Experimental behaviour of recycled aggregate concrete filled stainless steel tube stub columns and beams, *Thin-Walled Struct.* 66, 62–75. <https://doi.org/10.1016/j.tws.2013.01.017>.
- [21] Cortés-Puentes, W.L. Palermo, D. Abdulridha, A. Majeed, M. (2016). Compressive strength capacity of light gauge steel composite columns, *Case Stud. Constr. Mater.* 5, 64–78. <https://doi.org/10.1016/j.cscm.2016.08.001>.
- [22] Azad, M.A.K. (2017). Experimental Study on the Strength and Behaviour of Concrete Infilled Light Gauge Steel Square Columns.
- [23] Petrus, C. Abdul Hamid, H. Ibrahim, A. Parke, G. (2010). Experimental behaviour of concrete filled thin walled steel tubes with tab stiffeners, *J. Constr. Steel Res.* 66, 915–922. <https://doi.org/10.1016/j.jcsr.2010.02.006>.
- [24] Hunaiti, Y.M. (1997). STRENGTH OF COMPOSITE SECTIONS WITH FOAMED AND LIGHTWEIGHT AGGREGATE CONCRETE, *Journ Mater. Civ. Eng.* 58–61.
- [25] Ghannam, S. Al-Ani, H.R. Al-Rawi, O. (2010). Comparative study of load carrying capacity of steel tube columns filled with lightweight concrete and normal concrete, *Jordan J. Civ. Eng.* 4, 164–169.
- [26] Salgar, P.B. Patil, P.S. (2019). Experimental Investigation on Behavior of High-Strength Light weight Concrete-Filled Steel Tube Strut Under Axial Compression, *Ina. Lett.* 4, 207–214. <https://doi.org/10.1007/s41403-019-00077-7>.
- [27] Eurocode 4: Design of composite steel and concrete structures-Part 1-1: General rules and rules for buildings. 2004.
- [28] A.C.I.E. Bulletin, Aggregates for Concrete ACI Education Bulletin E1-07, *Concr. Constr.* (2007) 29.
- [29] ASTM, ASTM C 127-08: Standard Test Method for Density, Relative Density (Specific Gravity), and Absorption of Fine Aggregate, (2008) 1–7.
- [30] American Society for Testing and Materials, 176504562-ASTM-A370.pdf, (1992).
- [31] ACI 318. '318M–19: Building Code Requirements for Reinforced Concrete and Commentary'; ACI Committee: San Bernardino, CA, USA, 2019; p. 261.
- [32] D.S. Simulia, Abaqus 6.14 / Analysis User's Guide, ABAQUS 6.14 Anal. User's Guid. I (2014) 862.
- [33] Allouzi, R. Alkloub, A. Naghawi, H. Al-Ajarmeh, R. (2019). Fracture Modeling of Concrete in Plain and Reinforced Concrete Members, *Int. J. Civ. Eng.* 17, 1029–1042. <https://doi.org/10.1007/s40999-018-0353-5>.

Paper submitted: 15.01.2022.

Paper accepted: 17.04.2022.

This is an open access article distributed under the CC BY 4.0 terms and conditions.